COMMUNICATION

ChemComm
www.rsc.org/chemcomm

# First crystallographic signature of an acyclic peptide nanorod: molecular mechanism of nanorod formation by a self-assembled tetrapeptide†

**Debasish Haldar,[a] Arijit Banerjee,[a] Michael G. B. Drew,[b] Apurba Kumar Das[a] and Arindam Banerjee*[a]**

[a] *Department of Biological Chemistry, Indian Association for the Cultivation of Science, Jadavpur, Kolkata-700 032, India. E-mail: bcab@mahendra.iacs.res.in; Tel: +91 33 2473 5904*

[b] *Department of Chemistry, The University of Reading, Whiteknights, Reading RG6 6AD, UK*

*Received (in Cambridge, UK) 4th March 2003, Accepted 22nd April 2003*
*First published as an Advance Article on the web 13th May 2003*

**A terminally protected acyclic tetrapeptide Boc-Aib-Val-Aib-β-Ala-OMe 1 (Aib: α-aminoisobutyric acid, β-Ala: β-Alanine) self-assembles into a continuous hydrogen-bonded supramolecular helix with an average diameter of 10Å (1nm) starting from a double bend molecular conformation in crystals and further self-assembly of this supramolecular architecture leads to the formation of polydisperse nanorods of diameters 10–40 nm.**

Nanostructured materials have drawn a significant amount of attention due to their novel properties that are different from the bulk counterparts. Inorganic nanorods or wires are relatively common.[1] However, much less attention has been paid to nanorods composed of purely organic materials. Non-covalent self-assembly of biomolecular building blocks are particularly important in the fabrication of new materials,[2] with a wide range of applications in nanotechnology because of their potential utility as artificial ion channels or as transport vehicles in drug delivery systems.[3] Recently, Perutz *et al*. have established that amyloid fibers are water field nanotubes.[4] Prusiner *et al*. reported that nanostructured tubular parallel β-helices are the key element of scrapie prion protein plaques.[5] Ghadiri *et al.* have carried out pioneering work on the design and construction of open ended nanotubes by ring stacking of cyclic D,L- peptides as subunits[6] and they have also established that the properties of the outer surface and the internal diameter of peptide nanotubes can be adjusted simply by judicious selection of the amino acid side chain functionalities[7] and the number of amino acid residues present within the cyclic peptide ring respectively. Peptide-based diblock oligomers[8] and polyphenylene dendrimers[9] have been used to construct nanorods. Zhang *et al.* have successfully designed and constructed self-assembling amphiphilic surfactant-like acyclic peptides which form nanotubes and nanovesicles through aggregated β-sheet architectures.[10] Most of the rod-like nanostructures that have been discussed so far are composed of either cyclic peptides or rigid organic templates[11] and the rod-like character derives from the inherent rigidity of the molecular segments. However, the crystallographic signature of acyclic peptide nanostructure formation is very rare.[12] In this report the molecular folding of the tetrapeptide subunit directs the formation of a supramolecular helical structure, which eventually leads to the formation of a nanorod. Our previous studies demonstrated that oligopeptides can be designed to self-assemble into amyloid-like fibril forming supramolecular β-sheets.[13] Recently, our group have established the formation of supramolecular peptide helices from short peptide molecules.[14] Here, we elucidate the molecular mechanism of acyclic peptide nanorod formation through a hydrogen bonded supramolecular helix from a terminally protected tetrapeptide Boc-Aib(1)-Val(2)-Aib(3)-β-Ala(4)-OMe **1**. To the best of our knowledge this is the first crystallographic evidence of acyclic peptide nanorod formation from a tetrapeptide with non-coded amino acids.

The tetrapeptide subunit employed in the present study, Boc-Aib(1)-Val(2)-Aib(3)-β-Ala(4)-OMe **1**‡ is constructed from two conformationally constrained Aib (α-aminoisobutyric acid) residues in order to enhance the helical nature of the peptide backbone.[15] The structure of the peptide is shown in Figure 1 with the atomic numbering scheme. There are two successive intramolecular hydrogen bonds ($N_5$—H···$O_{12}$, $N_8$—H···$O_{15}$) resulting in a consecutive double bend conformation in the molecule in the crystalline state. The backbone torsion angle values of peptide **1** are available in the ESI.† The crystal structure reveals that there are two overlapping β-turns placing Aib(1)-Val(2) as corner residues for the first turn and Val(2)-Aib(3) as the corner residues for the next turn. The residue Val(2) simultaneously occupies the $i + 2$ position of the first turn and $i + 1$ for the succeeding turn. In the crystal, the individual peptide subunits are regularly aligned *via* multiple intermolecular hydrogen bonds to form highly ordered supramolecular helical assemblies around the screw axis parallel to crystallographic b axis (Figure 1 of the ESI†). The hydrogen bonding parameters of peptide **1** are listed in Table 1. The space-filling model of the supramolecular helix (Figure 2 of the ESI†) clearly demonstrates that the individual β-bend structures are stacked one on top of the other, maintaining proper registry between the subunits, generating a rod-like architecture with an average diameter of 10 Å. The self-assembly of this tetrapeptide molecule is mainly driven by directed hydrogen bonding interactions. The interior of the peptide supramolecular helical

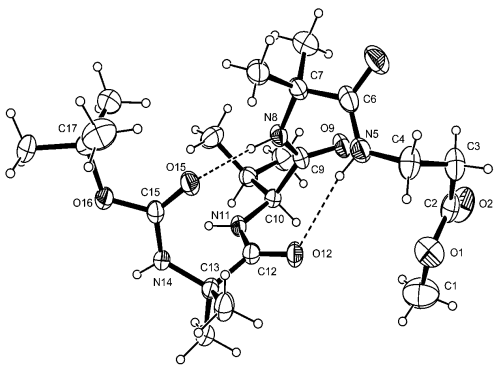


**Fig. 1** ORTEP diagram with atomic numbering scheme of the peptide **1**. Thermal ellipsoids are shown at 30% probability level. Intramolecular hydrogen bonds are shown as dotted lines.

**Table 1** Hydrogen bonding parameters of peptide **1**

| D–H···A | H···A (Å) | D···A (Å) | D–H···A (°) |
|---|---|---|---|
| N8–H8···O15 | 2.26 | 3.08 | 159.1 |
| N5–H5···O12 | 2.54 | 3.39 | 168.4 |
| N11–H11···O2[a] | 2.28 | 3.10 | 158.2 |
| N14–H14···O9[a] | 2.23 | 3.04 | 156.8 |

[a] Symmetry element $2 - x$, $0.5 + y$, $-0.5 - z$.

† Electronic supplementary information (ESI) available: selected backbone torsion angles for **1**, Figure showing packing of 1, and a space-filling model of higher-ordered supramolecular helical assembly of **1**. See http://www.rsc.org/suppdata/cc/b3/b302472p/

DOI: 10.1039/b302472p

 

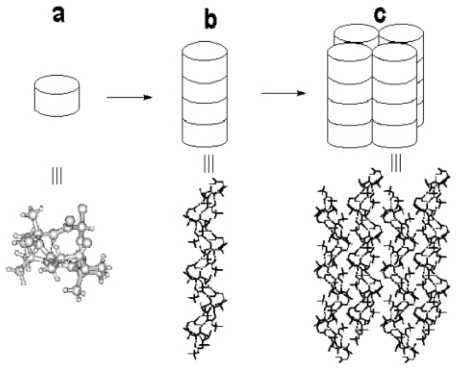


**Fig. 2** The schematic representation illustrates the stepwise self-assembly of the reported peptide into nanorods (a) the unimolecular folding nature showing double bend structure; (b) the unique supramolecular helical architecture which is formed mainly through intermolecular hydrogen bonding among the tetrapeptide subunits; (c) further self-assembly of individual peptide helices into nanorods which is mediated by noncovalent interactions other than hydrogen bonding. For clarity nonhydrogen bonded hydrogens are omitted. For the sake of simplicity only four self-associating supramolecular helical structures are shown.

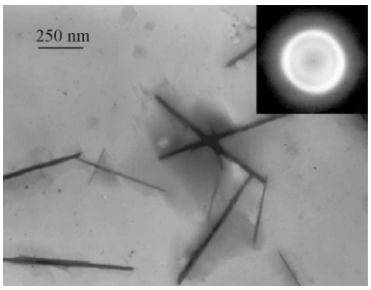


**Fig. 3** Electron microscopy and electron diffraction (0.5% w/v, camera length 0.8 m) of peptide **1**. Transmission electron micrographs of peptide **1** showing nanorod like morphology in the solid state. The sample was prepared on a carbon coated copper grid by slow evaporation of methanol–water solution of the peptide **1**.

structure is hydrophilic due to the presence of backbone –CONH– moieties, while the exterior is hydrophobic constructed from the side chains of Aib(1), Aib(3) and Val(2). Figure 2 provides a pictorial representation of the formation of nanorods by self-association of the acyclic peptide subunits through hydrogen bonding and other noncovalent interactions to form first a unique supramolecular helical structure which further self-assembles through non hydrogen-bonding noncovalent interactions to form nanorods of various diameters ranging from 10 nm to 40 nm.

Transmission electron microscopy of peptide **1** at high magnification provides a detailed structure of the peptide nanorods. It should be pointed out that under the TEM, only a two dimensional projection of the specimen could be imaged. The TEM image (Figure 3) reveals that the peptide **1** has formed nanorods with diameters ranging from 10 to 40 nm.

This report highlights a short acyclic terminally protected tetrapeptide subunit which has the propensity to form a unique supramolecular helix of an average diameter of 10 Å and further self-assembly of this supramolecular architecture leads to the formation of polydisperse nanorods of diameters ranging from 10 to 40 nm. Here, the nanorods are composed of a new bioorganic material, an acyclic peptide whose constituents are proteinous (Val) and natural non-proteinous amino acid (Aib and β-Ala) residues. Processes are being made to construct monodisperse acyclic peptide nanorods with some useful functionalities attached to the individual peptide subunits.

We thank EPSRC and University of Reading, U.K. for funds for the Image Plate System. We acknowledge the Department of Science and Technology, New Delhi, India for financial support.

## Notes and references

‡ The peptide **1** was synthesized by conventional solution phase method and characterized by $^1$H NMR spectroscopy and mass spectrometry. A colorless orthorhombic crystal, suitable for an X-ray diffraction study was obtained from ethyl acetate solution by slow evaporation.

*Crystal data for peptide* **1**: $C_{22}H_{40}N_4O_7$, M = 472.58, orthorhombic, $a$ = 9.167(15), $b$ = 15.61(2), $c$ = 19.07(3) Å, $U$ = 2729 Å$^3$, $T$ = 293 K, space group $P2_12_12_1$, $Z$ = 4, $d_m$ = 1.150 Mg m$^{-3}$. Intensity data were collected with MoKα radiation using the MARresearch Image Plate System. The crystal was positioned at 70 mm from the Image Plate. 100 frames were measured at 2° intervals with a counting time of 2 min to give 4787 independent reflections. Data analysis was carried out with the XDS program.[16] The structure was solved using direct method with the Shelx86 program.[17] The non-hydrogen atoms were refined with anisotropic thermal parameters. The hydrogen atoms were included in geometric positions and given thermal parameters equivalent to 1.2 × those of the atom to which they were attached. The structure was refined on $F^2$ using Shelxl.[18] The final $R$ values were $R_1$ 0.0662 and $wR_2$ 0.1659 for 2613 data with $I > 2\sigma(I)$. The largest peak and hole in the final difference Fourier were 0.190 and −0.212 e Å$^{-3}$. CCDC 205506. See http://www.rsc.org/suppdata/cc/b3/b302472p/ for crystallographic data in .cif or other electronic format.

1 (*a*) J. J. Urban, W. S. Yun, Q. Gu and H. Park, *J. Am. Chem. Soc.*, 2002, **124**, 1186; (*b*) X. Peng, L. Mann, W. Wang, J. Wickham, E. Sher, A. Kadvanich and A. P. Alivisators, *Nature*, 2002, **404**, 59; (*c*) L. Manna, E. C. Sher and A. P. Alivisators, *J. Am. Chem. Soc.*, 2000, **122**, 12700; (*d*) H. H. Huang, S. Mao, H. Feick, H. Yall, Y. Wu, H. Kind, E. Weber, R. Russo and P. Yang, *Science*, 2001, **292**, 1897; (*e*) M. S. Gudiksen and C. M. Lieber, *J. Am. Chem. Soc.*, 2000, **122**, 8801.

2 (*a*) G. M. Whetesides, J. P. Mathias and C. T. Seto, *Science*, 1991, **254**, 1312; (*b*) J. M. Lehn, *Science*, 1993, **260**, 1762; (*c*) D. T. Bong, T. D. Clark, J. R. Granja and M. R. Ghadiri, *Angew. Chem. Int. Ed.*, 2001, **40**, 988.

3 (*a*) J. R. Granja and M. R. Ghadiri, *J. Am. Chem. Soc.*, 1994, **116**, 10785; (*b*) Y. Tanaka, Y. Kobuke and M. Sokabe, *Angew. Chem. Int. Ed. Engl.*, 1995, **34**, 693; (*c*) M. R. Ghadiri, J. R. Granja, R. A. Milligran, D. E. McRee and N. Khazanovich, *Nature*, 1993, **366**, 324; (*d*) M. R. Ghadiri, J. R. Granja and L. K. Buehler, *Nature*, 1994, **369**, 301; (*e*) D. Marsh, *Biochem. J.*, 1996, **315**, 345.

4 M. F. Perutz, J. T. Finch, J. Berriman and A. Lesk, *Proc. Natl. Acad. Sci.*, 2002, **99**, 5591.

5 H. Wille, M. D. Michelitsch, V. Guenebaut, S. Supattapone, A. Serban, F. E. Cohen, D. A. Agard and S. B. Prusiner, *Proc. Natl. Acad. Sci.*, 2002, **99**, 3563.

6 (*a*) J. D. Hartgerink, T. D. Clark and M. R. Ghadiri, *Chem. Eur. J.*, 1998, **4**, 1367; (*b*) J. D. Hartgerink, J. R. Granja, R. A. Milligan and M. R. Ghadire, *J. Am. Chem. Soc.*, 1996, **118**, 43.

7 M. R. Ghadiri, K. Kobayashi, J. R. Granja, R. K. Chadha and D. E. McRee, *Angew. Chem. Int. Ed. Engl.*, 1995, **34**, 93.

8 (*a*) H. A. Klok, J. F. Langenwalter and S. Lccommandoux, *Macromolecules*, 2000, **33**, 7819; (*b*) J. D. Hartgerink, E. Beniash and S. I. Stupp, *Science*, 2001, **294**, 1684.

9 S. Loi, U. M. Wiesler, H. J. Butt and K. Müllen, *Chem. Commun.*, 2000, 1169.

10 S. Vauthey, S. Santoso, H. Gong, N. Watson and S. Zhang, *Proc. Natl. Acad. Sci.*, 2002, **99**, 5355.

11 (*a*) N. Sakai, N. Majumdar and S. Matile, *J. Am. Chem. Soc.*, 1999, **121**, 4294; (*b*) N. Sakai, K. C. Brennan, L. A. Weiss and S. Matile, *J. Am. Chem. Soc.*, 1997, **119**, 8726; (*c*) D. Ranganathan, V. Haridas, C. S. Sundari, P. Balasubramanium, K. P. Madhusudanan, R. Roy and I. L. Karle, *J. Org. Chem.*, 1999, **64**, 9230; (*d*) D. Ranganathan, C. Lakshmi and I. L. Karle, *J. Am. Chem. Soc.*, 1999, **121**, 6103.

12 C. H. Gorbitz, *Chem. Eur. J.*, 2001, **7**, 5153.

13 (*a*) S. K. Maji, M. G. B. Drew and A. Banerjee, *Chem. Commun.*, 2001, 1946; (*b*) A. Banerjee, S. K. Maji, M. G. B. Drew, D. Haldar and A. Banerjee, *Tetrahedron Lett.*, 2003, **44**, 335.

14 (*a*) D. Haldar, S. K. Maji, W. S. Sheldrick and A. Banerjee, *Tetrahedron Lett.*, 2002, **43**, 2653; (*b*) D. Haldar, S. K. Maji, M. G. B. Drew, A. Banerjee and A. Banerjee, *Tetrahedron Lett.*, 2002, **43**, 5465; (*c*) S. K. Maji, A. Banerjee, M. G. B. Drew, D. Haldar and A. Banerjee, *Tetrahedron Lett.*, 2002, **43**, 6759; (*d*) A. Banerjee, S. K. Maji, M. G. B. Drew, D. Haldar and A. Banerjee, *Tetrahedron Lett.*, 2003, **44**, 699.

15 I. L. Karle and P. Balaram, *Biochemistry*, 1990, **29**, 6747.

16 W. Kabsch, *J. Appl. Cryst.*, 1988, **21**, 916.

17 G. M. Sheldrick, *Acta Cryst. A*, 1990, **46**, 467.

18 G. M. Sheldrick, *SHELXL-97, Program for refinement of crystal structures*, University of Göttingen, Germany, 1997.